Aggregated Network for Massive MIMO CSI Feedback

Zhilin Lu, Hongyi He, Zhengyang Duan, Jintao Wang, *Senior Member, IEEE* and Jian Song, *Fellow, IEEE*

Abstract—In frequency division duplexing (FDD) mode, it is necessary to send the channel state information (CSI) from user equipment to base station. The downlink CSI is essential for the massive multiple-input multiple-output (MIMO) system to acquire the potential gain. Recently, deep learning is widely adopted to massive MIMO CSI feedback task and proved to be effective compared with traditional compressed sensing methods. In this paper, a novel network named ACRNet is designed to boost the feedback performance with network aggregation and parametric RuLU activation. Moreover, valid approach to expand the network architecture in exchange of better performance is first discussed in CSI feedback task. Experiments show that ACRNet outperforms loads of previous state-of-the-art feedback networks without any extra information.

Index Terms—Massive MIMO, CSI feedback, deep learning, aggregated network, group convolution, parametric ReLU.

I. INTRODUCTION

The massive multiple-input multiple-output (MIMO) is widely regarded as one of the key techniques in the fifth-generation wireless communication system. With larger antenna array, such system is able to boost both spectrum and energy efficiency [1]. The downlink channel state information (CSI) needs to be obtained at BS for precoding so that the MIMO system can acquire the performance gain. In frequency division duplexing (FDD) mode, downlink CSI is usually estimated at the user equipment (UE) and fed back to the BS due to the channel non-reciprocity. However, the dimension of CSI matrix is sharply increased in massive MIMO system. The bandwidth consumed by CSI feedback is therefore unacceptable.

To address the above challenge, the CSI matrix should be compressed before feedback to reduce the overhead. The traditional compressed sensing (CS) works poorly since the channel matrix is not sparse enough under large compression ratio [2]. On the other hand, deep learning (DL) has achieved great success in computer vision and signal processing. Specifically, DL based methods have dominated the image compression task, which motivates researchers to compress the CSI matrix with neural network (NN) as well.

The first DL based CSI feedback algorithm is CsiNet introduced in [2], which shows a tremendous superiority against traditional CS based methods. After that, many works try to solve the CSI feedback problem under different scenarios or with extra information. Time varying CSI feedback is considered in [3] using recurrent neural network (RNN). Correlation between uplink and downlink CSI is utilized in [4] and [5]. Besides, [6] and [7] adopt donoise module to deal with imperfect feedback link and non-ideal channel estimation, respectively. Multi-user cooperative feedback is considered in [8] while network safety against adversarial attack is improved in [9]. In addition, some end-to-end models are designed combining CSI feedback with channel estimation or beamforming [10], [11]. The DL based CSI feedback module is integrated into a new radio (NR) 5G system and proved to be effective in [12].

At the mean while, a series of works focus on novel network or pipeline design in order to enhance the performance under the fundamental feedback scenario. Multi-resolution aided CRNet achieves

The authors are with the Department of Electronic Engineering, Tsinghua University, and Beijing National Research Center for Information Science and Technology (BNRist), Beijing 100084, China. (e-mail: {luzl18, hehy18, duanzy18}@mails.tsinghua.edu.cn; {wangjintao, jsong}@tsinghua.edu.cn).

The key results of this paper can be reproduced with github repository https://github.com/Kylin9511/ACRNet.

better feedback performance with advanced training scheme in [13]. CsiNetPlus introduced in [14] reduces the feedback error with larger convolution kernel. Non-local block is proved to be practical for feedback task in DS-NLCsiNet [15]. Additionally, quantization of the compressed CSI feature is considered in [16] and [17] to further reduce the feedback overhead. Network pruning is used in [18] in order to reduce the network complexity. An extremely light weight binary neural network named BCsiNet is proposed in [19], achieving over $30\times$ memory saving and $2\times$ acceleration compared with original CsiNet [2]. Note that the majority of these network or pipeline designs are relatively universal and can be beneficial for more advanced feedback scenarios mentioned above.

In this paper, we design a novel neural network named aggregated channel reconstruction network (ACRNet) to further boost the performance of CSI feedback task under the fundamental scenario. The main contribution of this thesis is listed below.

- Inspired by ResNeXt [20], the proposed ACRNet takes the advantage of network aggregation and improves the quality of CSI feedback. Simulation shows that our proposed ACRNet outperforms a wide range of existing feedback networks and gives a state-of-the-art results.
- In this paper, we explore the best way of network expansion for CSI feedback task, so that better feedback performance can be easily exchanged with reasonable extra complexity. In general, we argue that width dilation with aggregation is a suitable technique for feedback network expansion to meet different resource limitations. To the best of the author's knowledge, we are the first to discuss effective ways of network expansion for CSI feedback task.
- Learnable activation function is applied in ACRNet and proved to be beneficial. Parametric rectified linear unit (PReLU) [21] allows different convolution channels to have their own activation parameters, which further increases the degree of freedom for feature extraction.

The rest of the paper is arranged as follows. Section II introduces the system model of CSI feedback. Section III explains the proposed ACRNet architecture in details. The numerical results and analysis are given in section IV and conclusion is drawn in section V.

II. SYSTEM MODEL

In this paper, a single cell massive MIMO system is adopted, where the BS has N_t transmitting antennas and the UE equips N_r receiving antennas. Note that $N_t \gg N_r$ and N_r is set to 1 for simplicity. An orthogonal frequency division multiplexing (OFDM) system with N_c sub-carrier is considered. The received signal y_n on the nth sub-carrier ($n \in \{1, 2, \cdots, N_c\}$) at UE can be expressed as follows:

$$y_n = \mathbf{h}_n^H \mathbf{p}_n x_n + z_n, \tag{1}$$

where $x_n \in \mathbb{C}$ and $z_n \in \mathbb{C}$ are the transmitted symbol and additive Gaussian noise on the nth sub-carrier. $\mathbf{h}_n \in \mathbb{C}^{N_t \times 1}$ is the downlink channel response vector and $\mathbf{p}_n \in \mathbb{C}^{N_t \times 1}$ is the corresponding precoding vector. Since the uplink and downlink channel is not symmetric, $\mathbf{h}_n$ has to be estimated at UE and fed back to BS. We can concatenate all the channel response vectors into an overall downlink channel matrix $\mathbf{H} = [\mathbf{h}_1, \mathbf{h}_2, \cdots, \mathbf{h}_{N_c}]^H$. It it obvious that $\mathbf{H}$ contains $2 \times N_c \times N_t$ float numbers, which is unacceptably large for direct feedback in massive MIMO system.

In order to reduce the size of the CSI matrix, we transfer $\mathbf{H}$ from the spatial-frequency domain to the angular-delay domain with discrete Fourier transform (DFT) as [13].

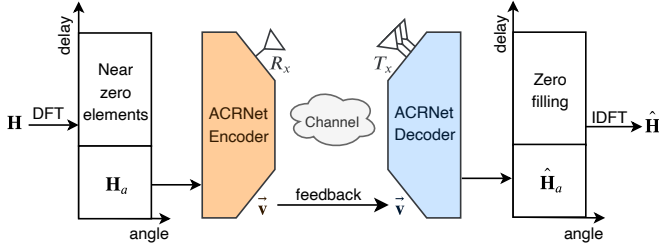$$\mathbf{H}' = \mathbf{F}_c \mathbf{H} \mathbf{F}_t^H, \tag{2}$$

Fig. 1. Overview of downlink CSI feedback pipeline. The CSI matrix is compressed by ACRNet encoder and reconstructed by ACRNet decoder.

where $\mathbf{F}_c \in \mathbb{C}^{N_c \times N_c}$ and $\mathbf{F}_t \in \mathbb{C}^{N_t \times N_t}$ are the DFT transform matrices respectively, while $\mathbf{H}'$ is the angular-delay domain CSI matrix. As depicted in Fig. 1, the majority of the elements in $\mathbf{H}'$ are zero or near-zero, which can be omitted during feedback. More precisely, only the first N_a row of $\mathbf{H}'$ contains large values since the time delays of all sub-carriers fall into a certain period. We truncate the first N_a row of $\mathbf{H}'$ and denote it as $\mathbf{H}_a$, which contains only $2 \times N_a \times N_t$ float numbers. By feeding back $\mathbf{H}_a$ instead of $\mathbf{H}$, the overhead can be largely reduced.

However, even $\mathbf{H}_a$ is too heavy for uplink feedback since N_t is large in massive MIMO system. Our purpose is to further compress matrix $\mathbf{H}_a$ to make the feedback as light as possible. In this paper, we follow the fundamental scheme proposed in [2]. The overview of the feedback pipeline is demonstrated in Fig. 1. The frequency-delay domain CSI matrix $\mathbf{H}_a$ is acquired with DFT and truncation. After that, the NN based CSI compression and recovery can be summarized as equation (3).

$$\hat{\mathbf{H}}_a = \mathcal{D}_{\mathrm{ACR}}(\mathcal{E}_{\mathrm{ACR}}(\mathbf{H}_a, \Theta_{\mathcal{E}}), \Theta_{\mathcal{D}}), \tag{3}$$

where $\mathcal{E}_{\mathrm{ACR}}$ and $\mathcal{D}_{\mathrm{ACR}}$ represent ACRNet encoder and decoder, while $\Theta_{\mathcal{E}}$ and $\Theta_{\mathcal{D}}$ stand for the learnable network parameter. Finally, the $\hat{\mathbf{H}}$ is reconstructed via zero filling and inverse DFT.

Notably, perfect uplink feedback of vector $\mathbf{v}$ is assumed and the CSI matrix is generated with COST2100 [22] channel model. Details of dataset simulation are given in section IV.

III. WIDE AGGREGATED FEEDBACK NETWORK DESIGN

A. The aggregated block design in ACRNet

The convolutional layer plays a significant role in neural network especially for computer vision task [23]. Since the CSI matrix can be viewed as an image depicting the physical layer channel pattern, almost all previous feedback networks are based on convolutional neural network (CNN) [2]–[5], [13]–[17].

Assume the dimension of the input feature map at the $(l-1)^{th}$ layer is $D_{in}H_{in}W_{in}$ and the dimension of the output feature map at the lth layer is $D_{out}H_{out}W_{out}$. The standard convolution without bias can be expressed as follows:

$$X_j^l = \sum_{i \in \mathbb{C}^{l-1}} X_i^{l-1} \circledast K_{ij}^{l-1}, \tag{4}$$

where X_i^{l-1} and X_j^l are the ith and j^{th} layer of the input and output feature map, respectively. K_{ij}^{l-1} represents the convolutional kernel with size $k \times k$, which connects feature map X_i^{l-1} and X_j^l. $\mathbb{C}^{l-1}$ is the set of input channel indices and $\circledast$ denotes the convolutional operation. Obviously, $|\mathbb{C}^{l-1}| = D_{in}$ for standard convolution and the corresponding flops is $D_{in} \times H_{out}W_{out}k^2 \times D_{out}$.

However, each output channel is related with all input channels in standard convolution. The computation is rather heavy and the

extracted features are highly correlated. In order to overcome these drawbacks, the aggregated network replaces standard convolution with group convolution in ResNeXt [20]. The group convolution can be described with equation (5).

$$X_j^l = \sum_{i \in \mathbb{G}_n^{l-1}} X_i^{l-1} \circledast K_{ij}^{l-1}, \tag{5}$$

where the only difference compared with (4) is the set of input channel indices $\mathbb{G}_n^{l-1}$ is a sub set of original $\mathbb{C}^{l-1}$. With g groups in total, we have $|\mathbb{G}_n^{l-1}| = D_{in}/g$ for $\forall n \in \{1, \cdots, g\}$. Therefore, the flops of the group convolution is $D_{in}/g \times H_{out}W_{out}k^2 \times D_{out}$, which is g times smaller than the standard convolution.

In ACRNet, we propose an aggregated block specially designed for CSI feedback task. As demonstrated in Fig. 2, the aggregated block adopts convolution factorization in [13] and splits the standard convolution into parallel groups to enrich the extracted CSI features, which can be realized with group convolution. The enriched CSI features reduce the overfitting and therefore boost the feedback performance. The number of channels in each group is always two, aligned with the original CSI matrix. As mentioned above, the aggregated block is much lighter than the standard block.

B. The expandable ACRNet architecture design

It is a common academic paradigm for neural network design to provide expandable architecture [20], [23]. For instance, ResNet18-half is suitable for real time inference on portable devices while ResNet101 is a better choice if the inference is offline on the GPU server. However, previous CSI feedback network designs have not considered the network expansion algorithms seriously. As a result, user might get confused about how to adjust the network architecture when their hardware resources are deficient or excessive.

In this paper, we design a new feedback network named ACRNet and provide an efficient way of network expansion for it. Generally speaking, there are two basic dimensions that can expand a given network, the depth and the width. As it is shown in Fig. 3, the depth expansion adds extra blocks in a serial way while the width expansion enlarges the number of channels in the existing blocks.

Due to the limited resources of the encoder at UE, the network expansion of ACRNet only enlarges the decoder. First of all, we argue that width expansion is more suitable for CSI feedback task compared with depth expansion. The feedback network is indeed an auto encoder for unsupervised learning, which aims at compressing and recovering the spatial information of the given CSI matrix. It is widely known that the semantic information becomes richer while
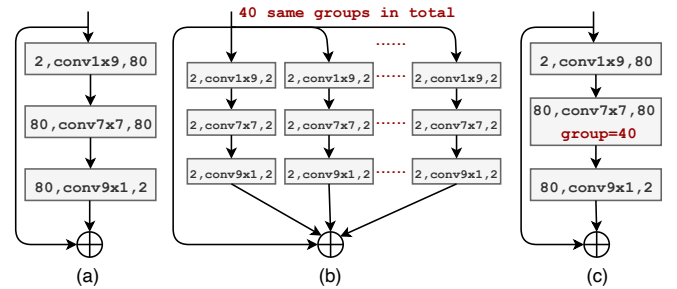

Fig. 2. Diagram of aggregated block design for CSI feedback in ACRNet-10×. The numbers at the beginning and the end of each convolution layer stand for the dimension of input and output channels. (a) stands for the standard block with normal convolution, while (b) represents the corresponding aggregated block in ACRNet-10× with 40 parallel groups. (c) is an equivalent realization of (b) with group convolution.
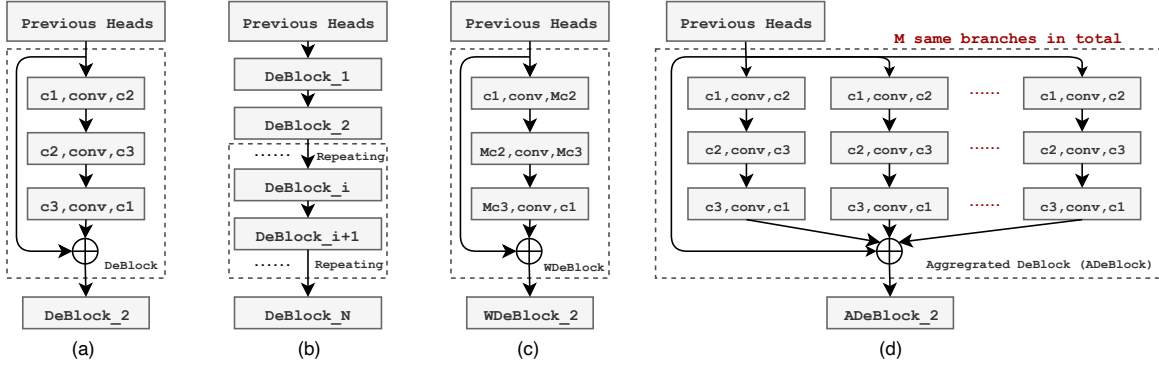
Fig. 3. General methods of network expansion. The digits at the beginning and the end of each convolution layer represent the number of input and output channels. The expansion focus on the decoder at BS since the encoder is resource sensitive. (a) is the original decoder to be expanded. (b) illustrates the depth expansion while (c) explains the width expansion. Finally (d) shows the width expansion on aggregated block, which is used in the proposed ACRNet.
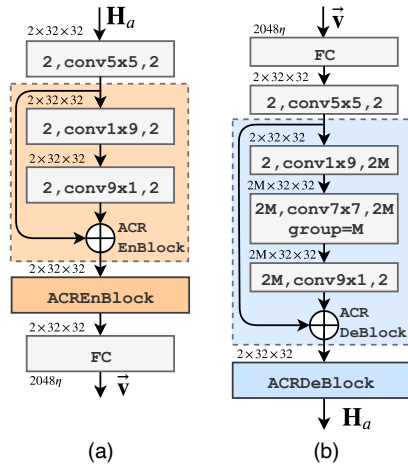

Fig. 4. The proposed ACRNet architecture. The shape of input feature map $c \times h \times w$ is given on the top of each block. Note that each convolution layer is followed by a batch normalization (BN) layer, and all activation functions and reshape layers are omitted for simplicity.

the spatial information becomes vaguer as the network goes deeper. Therefore making the network very deep might not a good choice for CSI feedback due to the loss of spatial information.

On the other hand, the width expansion can enrich the spatial information to boost the feedback performance. Specifically, width expansion is proved to be more efficient on aggregated block compared with normal block under the same complexity. Experiments show that pure width expansion on aggregated block is able to bring satisfactory feedback performance gain. It is worth mentioning that joint optimization of network width, depth, kernel size, multi-resolution branches [13], etc. can make the feedback network even more powerful. Such optimization is too complicated and might needs the help of neural architecture search (NAS) technique.

The overall ACRNet is depicted in Fig. 4. A 5×5 convolution head is followed by a pair of ACREnBlocks in ACRNet encoder. A FC layer compresses the extracted feature to the target dimension 2048η, where η is the compression ratio. For ACRNet decoder, an opposite FC layer restores the reduced dimension and another 5×5 convolution layer serves as the decoder head. Then comes two expandable ACRDeBlocks, which are the main contributor for CSI recovery. Users can enlarge the proposed ACRNet by simply increasing M in the ACRDeBlock.

The lightest ACRNet-$1\times$ sets M to 4, while the polyploid

ACRNet-$k\times$ amplifies the factor M to $4k$. For both ACREnBlock and ACRDeBlock, convolution factorization of 9×9 kernel is applied and residual structure is used. Note that batch normalization (BN) and activation are added at the end of each convolution layer.

C. The parametric ReLU activation

All activation layers in ACRNet adopt the PReLU function except the last one, which uses sigmoid function for range normalization. The PReLU activation can be expressed as follows.

$$\mathrm{PReLU}(x) = \begin{cases} x, & x \geq 0 \\ \alpha x, & x < 0, \end{cases} \tag{6}$$

where $\alpha \in \mathbb{R}$ is the learnable negative slope. Note that each output channel has an independent learnable α.

If we fix $\alpha = 0.3$, the PReLU activation will degenerate to the leaky ReLU (LReLU) used in previous works [2], [13], [14]. The comparison among vanilla ReLU, LReLU and PReLU is shown in Fig. 5. PReLU improves the feedback performance by offering more freedom for feature extraction, since each channel in feature map can learn its own ReLU negative slope.

IV. SIMULATION RESULTS AND ANALYSIS

A. Experimental settings

As many previous works, we follow the experimental settings used in [2]. Based on COST2100 channel model [22], the indoor scenario at 5.3GHz and the outdoor scenario at 300MHz are considered. FDD system with 1024 sub-carriers is adopted and N_a is set to 32. For massive MIMO system, uniform linear array (ULA) model is used with $N_t = 32$. The training and test dataset are independently generated with 100,000 and 20,000 CSI matrices, respectively.

As for the deep learning hyper-parameters, the batch size is 200 and the loss function is MSE. Adam optimizer is used with $\beta_1 =$
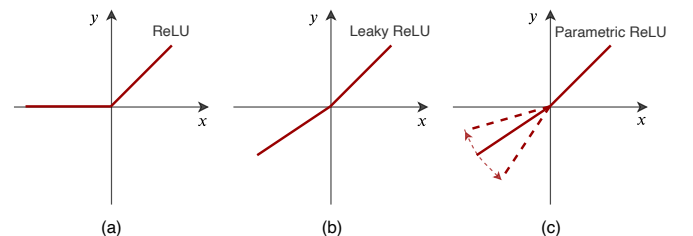

Fig. 5. Comparison of ReLU, Leaky ReLU and Parametric ReLU activation.

0.9 and $\beta_2 = 0.999$. We adopt the warm up aided cosine annealing scheduler introduced in [13], which can be derived as follows.

$$\text{lr} = \text{lr}_{min} + \frac{1}{2}\left(\text{lr}_{max} - \text{lr}_{min}\right)\left(1 + \cos\left(\frac{t - T_w}{T - T_w}\pi\right)\right), \quad (7)$$

where t stands for the index of current epoch and lr is the corresponding learning rate. The number of training epochs $T = 2500$ and the number of warm up epochs $T_w = 30$. the initial learning rate $\text{lr}_{max} = 4\text{e-}3$ while the minimal learning rate $\text{lr}_{min} = 5\text{e-}5$.

B. Performance of the expandable ACRNet

Generally, the performance of CSI feedback is measured by the normalized mean square error (NMSE) between the original angular-delay domain matrix $\mathbf{H}_a$ and the recovered one $\hat{\mathbf{H}}_a$.

$$\text{NMSE} = \mathbb{E}\left\{\frac{\|\mathbf{H}_a - \hat{\mathbf{H}}_a\|_2^2}{\|\mathbf{H}_a\|_2^2}\right\} \quad (8)$$

Table I shows the NMSE performance comparison between the proposed ACRNet and series of influential previous feedback networks. As we can see, the lightweight ACRNet-1× is lightest among them and provides decent NMSE, which outperforms the heavier CsiNet. More importantly, the expanded ACRNet-10× achieves state-of-the-art feedback performance with limited complexity for all compression ratio under both indoor and outdoor scenario.

The effectiveness of width expansion with aggregation is proved with experiments in Fig. 6. The network gradually fails to recover the CSI matrix due to the loss of spatial information brought by the

TABLE I
NMSE (dB) AND COMPLEXITY COMPARISON BETWEEN SERIES OF FEEDBACK NETWORKS AND PROPOSED EXPANDABLE ACRNet

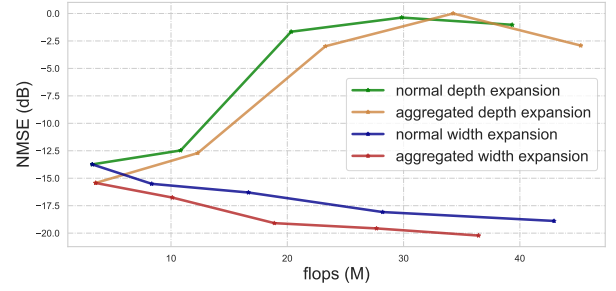| η	Methods	Complexity		NMSE[a]	
		flops	params	indoor	outdoor
1/4	CsiNet [2]	5.41M	2103K	-17.36	-8.75
	CRNet [13]	5.12M	2103K	-26.99	-12.70
	DS-NLCsiNet [15]	11.30M	2108K	-24.99	-12.09
	CsiNetPlus [14]	24.57M	2122K	-27.37	-12.40
	ACRNet-1× (ours)	**4.57M**	**2102K**	-25.62	-10.94
	ACRNet-10× (ours)	24.33M	2123K	**-28.89**	**-13.52**
1/8	CsiNet [2]	4.37M	1054K	-12.70	-7.61
	CRNet [13]	4.07M	1054K	-16.01	-8.04
	DS-NLCsiNet [15]	10.25M	1059K	-17.00	-7.96
	CsiNetPlus [14]	23.52M	1073K	-18.29	-8.72
	ACRNet-1× (ours)	**3.52M**	**1054K**	-15.43	-7.80
	ACRNet-10× (ours)	23.28M	1074K	**-19.61**	**-9.16**
1/16	CsiNet [2]	3.84M	530K	-8.65	-4.51
	CRNet [13]	3.55M	530K	-11.35	-5.44
	DS-NLCsiNet [15]	9.72M	534K	-12.93	-4.98
	CsiNetPlus [14]	23.00M	549K	-14.14	-5.73
	ACRNet-1× (ours)	**3.00M**	**529K**	-10.39	-5.17
	ACRNet-10× (ours)	22.76M	549K	**-14.70**	**-6.27**
1/32	CsiNet [2]	3.58M	268K	-6.24	-2.81
	CRNet [13]	3.28M	267K	-8.93	-3.51
	DS-NLCsiNet [15]	9.46M	272K	-8.64	-3.35
	CsiNetPlus [14]	22.74M	286K	-10.43	-3.4
	ACRNet-1× (ours)	**2.47M**	**267K**	-8.78	-3.36
	ACRNet-10× (ours)	22.50M	287K	**-10.59**	**-3.86**
1/64	CsiNet [2]	3.45M	137K	-5.84	-1.93
	CRNet [13]	3.16M	136K	-6.49	-2.22
	DS-NLCsiNet [15]	9.33M	141K	/	/
	CsiNetPlus [14]	22.61M	155K	/	/
	ACRNet-1× (ours)	**2.61M**	**136K**	-6.36	-2.16
	ACRNet-10× (ours)	22.36M	156K	**-7.44**	**-2.56**

[a] / means the performance is not reported.

Fig. 6. The complexity-performance trade off for four different network expansion methods. The experiments are based on the indoor scenario and the compression ratio is $\eta = 1/8$.

TABLE II
NMSE (dB) AND COMPLEXITY COMPARISON AMONG EXPANDABLE ACRNET VARIANTS

Methods	Complexity		NMSE[a]	
	flops	params	indoor	outdoor
ACRNet-1× (ours)	4.51M	2102K	-25.62	-10.94
ACRNet-4× (ours)	11.16M	2109K	-27.73	-12.71
ACRNet-8× (ours)	19.94M	2118K	-28.30	-13.32
ACRNet-12× (ours)	28.72M	2127K	-30.03	-13.84
ACRNet-16× (ours)	37.50M	2136K	**-30.98**	**-14.27**

[a] The compression ratio η is 1/4 for both indoor and outdoor.

increasing depth. What's more, width expansion based on aggregated block is proved to be more efficient compared with the normal block.

The feedback performances of series of ACRNet variants are given in Table II. It is clear that the larger the multiple of expansion is, the more precise the feedback will become. With reasonable extra complexity, the performance of the expanded ACRNet improves considerably, making the proposed expansion scheme an efficient trade-off when facing different resource limitations.

The comparison of the validation loss descending trend for CsiNet, CRNet and ACRNet variants is demonstrated in Fig. 7. We can see that the convergence of the ACRNet remains fast and stable with the expanding network and growing complexity.

C. Ablation study on activation functions

In this subsection, we present some ablation study on the activation function and analyze the distribution of learned negative slope α in
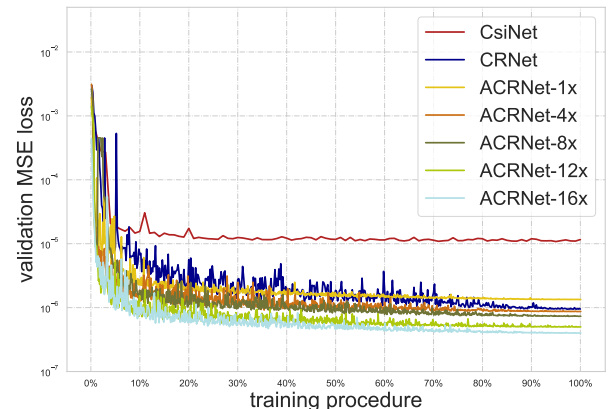

Fig. 7. The validation loss descending trend of CsiNet, CRNet and the proposed ACRNet variants.

TABLE III
NMSE (dB) COMPARISON ON DIFFERENT ACTIVATION FUNCTIONS

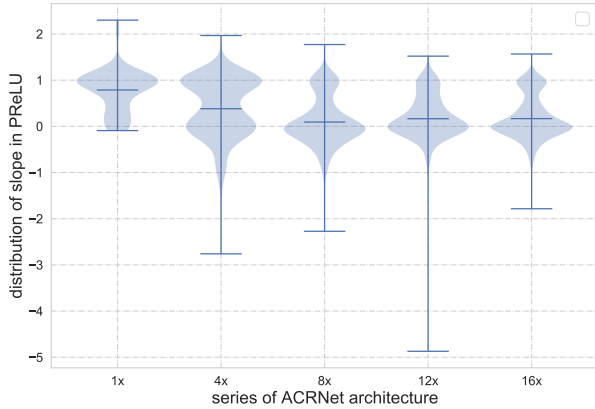| η	Scenario	Activation Scheme		
		LReLU	SPReLU	PReLU
1/4	indoor	-23.77	-24.75	**-25.62**
	outdoor	-10.21	-10.35	**-10.94**
1/8	indoor	-14.34	-13.78	**-15.43**
	outdoor	-7.07	-7.16	**-7.80**
1/16	indoor	-9.78	-10.07	**-10.39**
	outdoor	-5.00	-5.11	**-5.17**
1/32	indoor	-8.66	-8.55	**-8.78**
	outdoor	-3.17	-3.25	**-3.36**
1/64	indoor	-5.89	-6.24	**-6.36**
	outdoor	-2.13	-2.12	**-2.16**

Fig. 8. Distribution graph of the learned slope of PReLU for ACRNet variants. The three parallel lines represent the maximum, minimum and mean of the learned α. The shaded part shows the shape of probability distribution function (PDF) of α for each variant.

(6) in each ACRNet variants.

We use LReLU as short for original leaky ReLU and SPReLU as short for solely parametric ReLU, where each ReLU contains only one learnable α. The PReLU stands for the channel-wise parametric ReLU, where each output channel possesses different learnable α. Note that the PReLU activation the adopted one in the proposed ACRNet. The NMSE comparison among aforementioned activations is shown in Table III. It is obvious that the PReLU activation establishes superiority over the other schemes.

The distribution of the best learned α in each ACRNet variant is further studied in Fig. 8. When the network becomes heavier, the best mean of α seems to get closer to 0.2, which is not far from the 0.3 used in [2], [13]. In addition, local maxima of distribution appears at $\alpha = 1$ and $\alpha = 0$, which are absolute activation and ReLU activation, respectively. The combination of these two activation functions might be a better choice with less cost.

V. CONCLUSION

In this paper, a novel CSI feedback network named ACRNet was introduced for massive MIMO FDD system. The network aggregation technique and the PReLU activation were adopted and proved to be effective. Moreover, the network expansion scheme for CSI feedback task was first discussed, so that adequate performance gain could be acquired at the cost of reasonable extra complexity. Experiments showed that the proposed ACRNet greatly outperformed series of previous state-of-the-art networks including CRNet, DS-NLCsiNet and CsiNetPlus without any extra information.

REFERENCES

[1] L. Lu, G. Y. Li, A. L. Swindlehurst, A. Ashikhmin, and R. Zhang, "An overview of massive mimo: Benefits and challenges," *IEEE journal of selected topics in signal processing*, vol. 8, no. 5, pp. 742–758, 2014.

[2] C.-K. Wen, W.-T. Shih, and S. Jin, "Deep learning for massive mimo csi feedback," *IEEE Wireless Communications Letters*, vol. 7, no. 5, pp. 748–751, 2018.

[3] T. Wang, C.-K. Wen, S. Jin, and G. Y. Li, "Deep learning-based csi feedback approach for time-varying massive mimo channels," *IEEE Wireless Communications Letters*, vol. 8, no. 2, pp. 416–419, 2018.

[4] Z. Liu, L. Zhang, and Z. Ding, "Exploiting bi-directional channel reciprocity in deep learning for low rate massive mimo csi feedback," *IEEE Wireless Communications Letters*, vol. 8, no. 3, pp. 889–892, 2019.

[5] Y. Yang, F. Gao, G. Y. Li, and M. Jian, "Deep learning-based downlink channel prediction for fdd massive mimo system," *IEEE Communications Letters*, vol. 23, no. 11, pp. 1994–1998, 2019.

[6] H. Ye, F. Gao, J. Qian, H. Wang, and G. Y. Li, "Deep learning based denoise network for csi feedback in fdd massive mimo systems," *IEEE Communications Letters*, 2020.

[7] Y. Sun, W. Xu, L. Fan, G. Y. Li, and G. K. Karagiannidis, "Ancinet: An efficient deep learning approach for feedback compression of estimated csi in massive mimo systems," *IEEE Wireless Communications Letters*, 2020.

[8] J. Guo, X. Yang, C.-K. Wen, S. Jin, and G. Y. Li, "Dl-based csi feedback and cooperative recovery in massive mimo," *arXiv preprint arXiv:2003.03303*, 2020.

[9] Q. Liu, J. Guo, C.-K. Wen, and S. Jin, "Adversarial attack on dl-based massive mimo csi feedback," *arXiv preprint arXiv:2002.09896*, 2020.

[10] T. Chen, J. Guo, C.-K. Wen, S. Jin, G. Y. Li, X. Wang, and X. Hou, "Deep learning for joint channel estimation and feedback in massive mimo systems," *arXiv preprint arXiv:2011.07242*, 2020.

[11] J. Guo, C.-K. Wen, and S. Jin, "Deep learning-based csi feedback for beamforming in single-and multi-cell massive mimo systems," *arXiv preprint arXiv:2011.06099*, 2020.

[12] E. Zimaglia, D. G. Riviello, R. Garello, and R. Fantini, "A novel deep learning approach to csi feedback reporting for nr 5g cellular systems," in *2020 IEEE Microwave Theory and Techniques in Wireless Communications (MTTW)*, vol. 1. IEEE, 2020, pp. 47–52.

[13] Z. Lu, J. Wang, and J. Song, "Multi-resolution csi feedback with deep learning in massive mimo system," in *ICC 2020-2020 IEEE International Conference on Communications (ICC)*. IEEE, 2020, pp. 1–6.

[14] J. Guo, C.-K. Wen, S. Jin, and G. Y. Li, "Convolutional neural network-based multiple-rate compressive sensing for massive mimo csi feedback: Design, simulation, and analysis," *IEEE Transactions on Wireless Communications*, vol. 19, no. 4, pp. 2827–2840, 2020.

[15] X. Yu, X. Li, H. Wu, and Y. Bai, "Ds-nlcsinet: Exploiting non-local neural networks for massive mimo csi feedback," *IEEE Communications Letters*, 2020.

[16] C. Lu, W. Xu, S. Jin, and K. Wang, "Bit-level optimized neural network for multi-antenna channel quantization," *IEEE Wireless Communications Letters*, vol. 9, no. 1, pp. 87–90, 2019.

[17] Q. Yang, M. B. Mashhadi, and D. Gündüz, "Deep convolutional compression for massive mimo csi feedback," in *2019 IEEE 29th international workshop on machine learning for signal processing (MLSP)*. IEEE, 2019, pp. 1–6.

[18] J. Guo, J. Wang, C.-K. Wen, S. Jin, and G. Y. Li, "Compression and acceleration of neural networks for communications," *IEEE Wireless Communications*, vol. 27, no. 4, pp. 110–117, 2020.

[19] Z. Lu, J. Wang, and J. Song, "Binary neural network aided csi feedback in massive mimo system," *arXiv preprint arXiv:2011.02692*, 2020.

[20] S. Xie, R. Girshick, P. Dollár, Z. Tu, and K. He, "Aggregated residual transformations for deep neural networks," in *Proceedings of the IEEE conference on computer vision and pattern recognition*, 2017, pp. 1492–1500.

[21] K. He, X. Zhang, S. Ren, and J. Sun, "Delving deep into rectifiers: Surpassing human-level performance on imagenet classification," in *Proceedings of the IEEE international conference on computer vision*, 2015, pp. 1026–1034.

[22] L. Liu, C. Oestges, J. Poutanen, K. Haneda, P. Vainikainen, F. Quitin, F. Tufvesson, and P. De Doncker, "The cost 2100 mimo channel model," *IEEE Wireless Communications*, vol. 19, no. 6, pp. 92–99, 2012.

[23] K. He, X. Zhang, S. Ren, and J. Sun, "Deep residual learning for image recognition," in *Proceedings of the IEEE conference on computer vision and pattern recognition*, 2016, pp. 770–778.